

The relationship between cooling flows and metallicity measurements for X-ray luminous clusters.

S.W. Allen and A.C. Fabian

Institute of Astronomy, Madingley Road, Cambridge CB3 0HA

March 23, 2021

ABSTRACT

We explore the relationship between the metallicity of the intracluster gas in clusters of galaxies, determined by X-ray spectroscopy, and the presence of cooling flows. Using ASCA spectra and ROSAT images, we demonstrate a clear segregation between the metallicities of clusters with and without cooling flows. On average, cooling-flow clusters have an emission-weighted metallicity a factor ~ 1.8 times higher than that of non-cooling flow systems. We suggest this to be due to the presence of metallicity gradients in the cooling flow clusters, coupled with the sharply peaked X-ray surface brightness profiles of these systems. Non-cooling flow clusters have much flatter X-ray surface brightness distributions and are thought to have undergone recent merger events which may have mixed the central high-metallicity gas with the surrounding less metal-rich material. We find no evidence for evolution in the emission-weighted metallicities of clusters within $z \sim 0.3$.

Key words: galaxies: clusters: general – cooling flows – intergalactic medium – X-rays: galaxies

1 INTRODUCTION

X-ray spectroscopy provides an accurate measure of the metallicity of the hot intracluster medium (ICM) in clusters of galaxies. The strengths of the various emission lines relative to the continuum reveal the abundances of the emitting elements relative to hydrogen. Such measurements are particularly clear for the case of iron in rich clusters where the K-shell lines are typically well-defined in the X-ray spectra. The mass of the ICM dominates over the visible mass in stars in a cluster by a factor of 2–5 (Arnaud *et al.* 1992; David, Jones & Forman 1995; White & Fabian 1995). Metallicity measurements from X-ray observations thus provide firm constraints on the history of metal production within the cluster potential wells.

For low-redshift clusters, the observed abundance of iron in the ICM is approximately 1/3 solar (*e.g.* Edge & Stewart 1991). The strong correlation between the mass of iron and the total optical light from elliptical and lenticular galaxies within a cluster suggests that early-type galaxies are responsible for the bulk of the enrichment (Arnaud 1992). Mushotzky *et al.* (1996) showed that the relative abundances of individual elements such as Si, S and Fe determined from X-ray spectra suggest that most of the metals originate from type II supernovae. Mushotzky and Lowenstein (1997) further demonstrated that the iron abundance in rich clusters shows little evolution between $z \sim 0.3$ and now, suggesting that most of the enrichment of the ICM occurred at

high redshifts ($z > 0.3$). This is consistent with current semi-analytic models of galaxy formation (*e.g.* Kauffmann & Charlot 1997) which find that more than 80 per cent of the metal enrichment occurs at $z > 1$.

X-ray observations of clusters of galaxies show that in the central regions of most (70 – 90 per cent) clusters the cooling time of the ICM is significantly less than the Hubble time (Edge *et al.* 1992; Peres *et al.* 1997). The observed cooling leads to a slow net inflow of material towards the cluster centre; a process known as a cooling flow (Fabian 1994). The X-ray imaging data show that gas typically ‘cools out’ throughout the central few tens to hundreds of kpc in the clusters. Recent spatially resolved X-ray spectroscopy has confirmed the presence of distributed cool (and rapidly cooling) gas in cooling flows, with a spatial distribution and luminosity in excellent agreement with the predictions from the imaging data (Allen & Fabian 1997). The cooling flow in an X-ray luminous cluster can account for up to ~ 70 per cent of the total bolometric luminosity of the system (about half of this luminosity being due to material cooling out of the flow, and the rest due to the gravitational work done on the gas as it flows inwards; Allen *et al.* 1998).

Where abundance measurements have been compiled for large samples of clusters, a significant dispersion in the metallicity (which is primarily determined from the iron abundance) for clusters of a fixed X-ray luminosity and/or temperature has been revealed. In particular, the metallicity appears to depend on whether or not a cluster has a cool-

arXiv:astro-ph/9802219v2 2 Mar 1998

ing flow (Yamashita 1992; Fabian *et al.* 1994a) in the sense that cooling-flow clusters tend to have higher metallicities. Fabian *et al.* (1994a) speculated that this may be due to differences in the origins of the clusters, to the intracluster gas in the cooling-flow clusters being inhomogeneous with the cooler gas being more metal-rich, or due to the presence of metallicity gradients in these systems. Those clusters without cooling flows are assumed to have experienced a major merger event which has mixed the gas, leading to a lower *emission-weighted* metallicity.

In this paper we present metallicity measurements for a sample of 30 X-ray luminous clusters observed with ASCA and ROSAT (see Allen *et al.* 1998 for details). We identify the cooling flows in the sample and explicitly account for the effects of the cooling gas on the X-ray spectra. We argue that an abundance gradient in the cooling flow clusters underlies the variation seen in the emission-weighted metallicities. Throughout this paper, we assume $H_0=50 \text{ km s}^{-1} \text{ Mpc}^{-1}$, $\Omega = 1$ and $\Lambda = 0$.

2 OBSERVATIONS AND DATA ANALYSIS

Full details of the reduction and analysis of the total sample of 30 clusters are given in Allen *et al.* (1998). ROSAT High Resolution Imager (HRI) images were used to map the X-ray surface brightness profiles of the cluster cores and determine whether the individual clusters have cooling flows or not. The ASCA spectra were then fitted with a series of appropriate spectral models (see below) from which the metallicity measurements were made.

For the purposes of this paper, we have classified the clusters into subsamples of cooling-flow (CF) and non-cooling flow (NCF) systems. CFs are those clusters for which the upper (90 per cent confidence) limit to the central cooling time, as determined from a deprojection analysis of the ROSAT HRI X-ray images, is less than 10^{10} yr. NCFs are those systems with upper limits to their central cooling times $> 10^{10}$ yr. [The ‘central’ cooling time is the mean cooling time of the cluster gas in the innermost bin included in the deprojection analysis, which is of variable size (see Allen *et al.* 1998 for details). The use of a fixed physical size of 100 kpc for the central bin leads to very similar results (see Table).] Using this simple classification we identify 21 CFs and 9 NCFs in our sample. The mean redshift for the subsamples of both CF and NCF clusters is $\bar{z} = 0.21$.

The modelling of the ASCA spectra was carried out using the XSPEC spectral fitting package (version 9.0; Arnaud 1996). The spectra were modelled using the plasma codes of Kaastra & Mewe (1993; incorporating the Fe L calculations by Liedhal in XSPEC version 9.0) and the photoelectric absorption models of Balucinska-Church & McCammon (1992). The data from all four ASCA detectors were analysed simultaneously with the fit parameters linked to take the same values across the data sets. The exceptions were the emission measures of the ambient cluster gas in the four detectors which, due to the different extraction radii used, were allowed to fit independently.

Three models were fitted to the spectra. Model A, consisted of an isothermal plasma in collisional equilibrium, at the optically-determined redshift for the cluster, and absorbed by the nominal Galactic column density (Dickey &

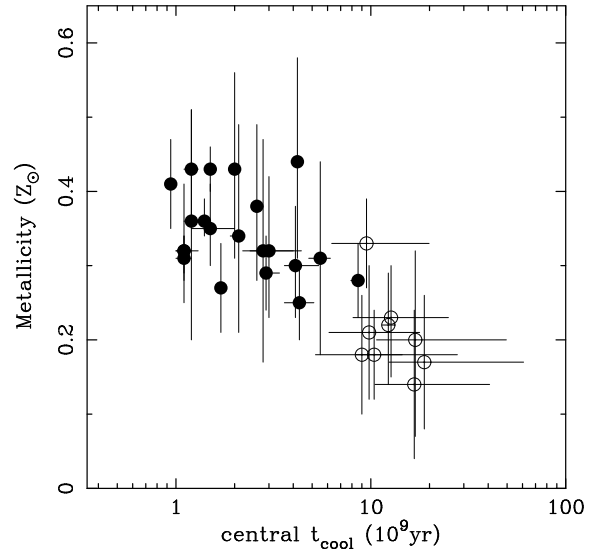


Figure 1. The emission-weighted metallicity of the cluster gas (determined with spectral model A) versus the central cooling time (from the deprojection analysis of the ROSAT HRI images). CFs are plotted as filled circles and non-cooling flows as open symbols. The figure illustrates a clear segregation in the mean emission-weighted metallicities for CF and NCF clusters.

Lockman 1990). The free parameters in this model were the temperature (kT) and metallicity (Z) of the plasma and the emission measures in the four detectors. (The metallicities are determined relative to the solar values of Anders & Grevesse (1989) with the different elements assumed to be present in solar ratios.) Secondly, model B, which was identical to model A but with the absorbing column density (N_H) also included as a free parameter in the fits. Thirdly, model C, which included an additional component explicitly accounting for the emission from the cooling flows in the clusters. The material in the cooling flows is assumed to cool at constant pressure from the ambient cluster temperature, following the prescription of Johnstone *et al.* (1992). The normalization of the cooling-flow component is parameterized in terms of a mass deposition rate, \dot{M} , which was free parameter in the fits. (The metallicity of the cooling gas was assumed to be equal to that of the ambient ICM.) The cooling flows were also assumed to be absorbed by an intrinsic column density, ΔN_H (Allen & Fabian 1997 and references therein), which was a further free parameter in the fits. The metallicity of X-ray absorbing material was fixed at the solar value (Anders & Grevesse 1989).

3 THE METALLICITY MEASUREMENTS

The metallicity measurements for the clusters are summarized in the Table. For the CF clusters we list the results obtained both with spectral models A and C (*i.e.* with and without the emission from the cooling flows accounted for in the spectral analysis). For the NCFs only the results for model A are listed.

Table 1. Summary of the cooling time, metallicity and baryon fraction measurements

	z	t_{cool} (10^9 yr)		Metallicity (solar)		$M_{\text{gas}}/M_{\text{total}}$ (at 500 kpc)
COOLING FLOWS						
		Central	100 kpc	MODEL A	MODEL C	MODEL C
Abell 478	0.088	$1.1^{+0.1}_{-0.1}$	3.11	$0.32^{+0.02}_{-0.03}$	$0.35^{+0.03}_{-0.04}$	$0.22^{+0.03}_{-0.03}$
Abell 586	0.171	$5.5^{+0.7}_{-0.7}$	7.94	$0.31^{+0.13}_{-0.13}$	$0.36^{+0.16}_{-0.15}$	$0.10^{+0.06}_{-0.05}$
PKS0745-191	0.103	$1.1^{+0.1}_{-0.1}$	2.65	$0.31^{+0.03}_{-0.03}$	$0.35^{+0.04}_{-0.03}$	$0.20^{+0.03}_{-0.03}$
IRAS 09104+4109	0.442	$2.0^{+0.1}_{-0.1}$	2.32	$0.43^{+0.13}_{-0.12}$	$0.51^{+0.17}_{-0.15}$	$0.12^{+0.03}_{-0.05}$
Abell 963	0.206	$4.1^{+1.3}_{-0.5}$	5.60	$0.30^{+0.08}_{-0.07}$	$0.31^{+0.07}_{-0.13}$	$0.21^{+0.03}_{-0.02}$
Zwicky 3146	0.291	$1.7^{+0.1}_{-0.1}$	2.53	$0.27^{+0.06}_{-0.06}$	$0.33^{+0.07}_{-0.06}$	$0.16^{+0.05}_{-0.05}$
Abell 1068	0.139	$1.2^{+0.1}_{-0.1}$	2.75	$0.43^{+0.08}_{-0.08}$	$0.42^{+0.10}_{-0.08}$	$0.17^{+0.04}_{-0.03}$
Abell 1413	0.143	$8.6^{+0.6}_{-0.7}$	8.63	$0.28^{+0.05}_{-0.05}$	$0.30^{+0.06}_{-0.05}$	$0.10^{+0.01}_{-0.01}$
Abell 1689	0.184	$2.9^{+0.5}_{-0.2}$	4.34	$0.29^{+0.05}_{-0.05}$	$0.30^{+0.06}_{-0.05}$	$0.18^{+0.01}_{-0.02}$
Abell 1704	0.216	$2.1^{+0.1}_{-0.2}$	3.59	$0.34^{+0.15}_{-0.13}$	$0.38^{+0.17}_{-0.16}$	$0.21^{+0.06}_{-0.08}$
RXJ1347.5-1145	0.451	$2.6^{+0.2}_{-0.1}$	3.00	$0.38^{+0.11}_{-0.10}$	$0.43^{+0.11}_{-0.11}$	$0.09^{+0.06}_{-0.02}$
Abell 1795*	0.063	$1.4^{+0.1}_{-0.1}$	3.42	$0.36^{+0.03}_{-0.02}$	$0.36^{+0.03}_{-0.02}$	$0.23^{+0.01}_{-0.01}$
MS1358.4+6245	0.327	$2.8^{+1.2}_{-0.6}$	4.76	$0.32^{+0.15}_{-0.15}$	$0.38^{+0.16}_{-0.15}$	$0.17^{+0.06}_{-0.08}$
Abell 1835	0.252	$1.5^{+0.5}_{-0.3}$	2.44	$0.35^{+0.06}_{-0.05}$	$0.40^{+0.06}_{-0.06}$	$0.24^{+0.03}_{-0.04}$
MS1455.0+2232	0.258	$1.1^{+0.2}_{-0.1}$	2.15	$0.32^{+0.09}_{-0.07}$	$0.37^{+0.09}_{-0.08}$	$0.26^{+0.05}_{-0.09}$
Abell 2029	0.077	$1.5^{+0.1}_{-0.1}$	3.54	$0.43^{+0.03}_{-0.03}$	$0.46^{+0.03}_{-0.03}$	$0.18^{+0.01}_{-0.02}$
Abell 2142	0.089	$4.3^{+0.8}_{-0.7}$	5.38	$0.25^{+0.05}_{-0.05}$	$0.27^{+0.05}_{-0.05}$	$0.18^{+0.01}_{-0.03}$
Abell 2204	0.152	$0.94^{+0.04}_{-0.04}$	2.01	$0.41^{+0.06}_{-0.06}$	$0.46^{+0.07}_{-0.07}$	$0.20^{+0.02}_{-0.04}$
Abell 2261	0.224	$3.0^{+1.4}_{-0.6}$	5.63	$0.32^{+0.10}_{-0.09}$	$0.37^{+0.09}_{-0.09}$	$0.13^{+0.04}_{-0.04}$
MS2137.3-2353	0.313	$1.2^{+0.1}_{-0.1}$	1.65	$0.44^{+0.14}_{-0.13}$	$0.50^{+0.15}_{-0.14}$	$0.21^{+0.03}_{-0.05}$
Abell 2390	0.233	$4.2^{+0.3}_{-0.2}$	5.45	$0.36^{+0.15}_{-0.16}$	$0.40^{+0.18}_{-0.16}$	$0.15^{+0.07}_{-0.08}$
MEAN	0.21 ± 0.11	2.61 ± 1.89	3.95 ± 1.91	0.344 ± 0.057	0.381 ± 0.065	0.177 ± 0.048
NON-COOLING FLOWS						
		Central	100 kpc	MODEL A		MODEL A
Abell 2744	0.308	$18.8^{+42.0}_{-6.4}$	19.2	$0.17^{+0.09}_{-0.09}$	—	$0.15^{+0.02}_{-0.01}$
Abell 520	0.203	$16.7^{+24.0}_{-6.2}$	16.3	$0.14^{+0.10}_{-0.10}$	—	$0.15^{+0.03}_{-0.02}$
Abell 665	0.182	$12.3^{+0.9}_{-0.9}$	13.0	$0.22^{+0.07}_{-0.08}$	—	$0.12^{+0.01}_{-0.01}$
Abell 773	0.217	$9.8^{+13.7}_{-6.6}$	11.2	$0.21^{+0.09}_{-0.09}$	—	$0.11^{+0.02}_{-0.02}$
Abell 2163	0.208	$12.7^{+12.3}_{-4.6}$	12.1	$0.23^{+0.07}_{-0.08}$	—	$0.13^{+0.01}_{-0.01}$
Abell 2218	0.175	$10.4^{+4.1}_{-2.0}$	12.8	$0.18^{+0.06}_{-0.06}$	—	$0.14^{+0.02}_{-0.02}$
Abell 2219	0.228	$9.0^{+18.8}_{-3.8}$	10.7	$0.18^{+0.08}_{-0.08}$	—	$0.15^{+0.01}_{-0.02}$
Abell 2319	0.056	$9.5^{+10.4}_{-3.2}$	9.81	$0.33^{+0.06}_{-0.06}$	—	$0.12^{+0.01}_{-0.01}$
AC114	0.312	$16.9^{+32.7}_{-6.2}$	16.6	$0.20^{+0.12}_{-0.13}$	—	$0.10^{+0.01}_{-0.02}$
MEAN	0.21 ± 0.08	12.90 ± 3.68	13.52 ± 3.15	0.207 ± 0.054		0.130 ± 0.019

NOTES: Column 2 lists the redshifts for the clusters. Columns 3 and 4 list the central cooling times and the mean cooling times within 100 kpc of the cluster centres determined from the deprojection analysis of the ROSAT HRI images. Columns 5 and 6 summarize the metallicity measurements for the clusters from the ASCA data using both the isothermal spectral model (A) and, for the CF clusters, the more sophisticated model incorporating the cooling-flow emission component (model C). Column 7 lists the ratios of the X-ray gas mass to the total mass at a radius of 500 kpc in the clusters. The errors on the central cooling times are the 10 and 90 percentile values determined from 100 Monte Carlo simulations in the deprojection analysis. Errors on the metallicity results and baryon fractions are 90 per cent ($\Delta\chi^2 = 2.71$) confidence limits. Errors on the mean values are the standard deviations of the distributions.

The results listed in the Table demonstrate a clear segregation between the metallicities of the CF and NCF clusters. For the CF systems, the mean metallicity determined with spectral model A is 0.34. For the NCFs, the mean value determined with the same spectral model is 0.21. The application of a Student's t-test (accounting for the possibility of unequal variances in the two distributions; Press *et al.* 1992) indicates that the mean metallicities for the CF and NCF clusters (determined using spectral model A) differ at $\gg 99.9$ per cent confidence. (The probability that the means of the two distributions are equal is 1.1×10^{-5} .) Note, however, that an F-test (Press *et al.* 1992) indicates the variances of the two distributions to be consistent at the 91 per cent confidence level.

For the CF clusters, the metallicities determined with spectral model C, which incorporates the cooling-flow component, are slightly higher ($Z_{\text{CF}} = 0.38$) than those inferred with spectral model A. The use of the cooling-flow model, where appropriate, therefore only enhances the discrepancy between the metallicities of the CF and NCF clusters. (The probability that the mean metallicities for the CF clusters, determined with spectral model C, and for the NCFs, determined with spectral model A, are equal is only 4.3×10^{-7} .) We note that the use of spectral model B in place of model A (*i.e.* allowing the absorbing column density acting on the clusters to be a free parameter in the fits) leads to very similar results.

The mean metallicity for the whole sample of 30 clusters, determined with spectral model A, is $\bar{Z} = 0.303 \pm 0.085$. If spectral model C is used for the CF clusters, the overall sample mean rises to $\bar{Z} = 0.329 \pm 0.102$. The mean metallicity measured with model A is in good agreement with the value of $\bar{Z} = 0.27 \pm 0.15$ determined by Edge & Stewart (1991), from EXOSAT observations of low-redshift clusters (using a similar spectral model. This value has been adjusted to account for the different Fe/H ratio assumed in that study.) For individual clusters, our results also show good agreement with those of Yamashita (1992), from GINGA observations, after correction for the different definition of solar metallicity used in that work. The standard deviations in the metallicity measurements for the subsamples of CF and NCF clusters (5.7×10^{-2} and 6.5×10^{-2} for the CFs with models A and C, respectively, and 5.4×10^{-2} for the NCFs with model A) are smaller, by a factor of ~ 2 , than that for the sample as a whole, and are more in line with expectations from theoretical models (*e.g.* Kauffmann & Charlot 1997).

We note that Abell 2319 is the only NCF-classified cluster with a metallicity comparable to that of a CF system. This is probably due to our conservative approach in classifying systems as NCFs. Abell 2319 is the only NCF in the Table with a mean cooling time within 100 kpc of the cluster centre of less than 10^{10} yr. Further observations will clarify the identification of Abell 2319 as a CF or NCF cluster.

Sixteen of the clusters included in our study (11 CFs and 5 NCFs) are also included in the study of Mushotzky & Lowenstein (1997). However, these authors only included a cooling-flow component in the spectral analysis for two of the eleven CF clusters in their sample (Zwicky 3146 and Abell 2390). In general, our results show good agreement with those of Mushotzky & Lowenstein (1997), although our values for a few of the CF clusters are slightly higher. This

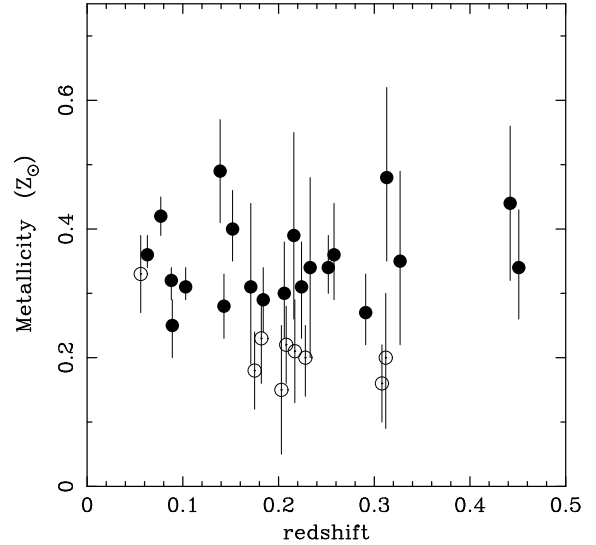


Figure 2. The metallicity measurements for the clusters (determined using spectral model A) as a function of redshift. The figure illustrates a lack of evolution in the emission-weighted metallicities of clusters within $z \sim 0.3$.

is presumably due to recent improvements in the calibration of the the ASCA instruments.

We have searched for evidence of evolution in the cluster metallicities by splitting the clusters into two subsamples, with redshifts less and greater than the mean value of $z = 0.210$. This gives 16 clusters with $z < 0.210$ (mean redshift 0.14) and 14 with $z > 0.210$ (mean redshift 0.29), with an approximately even mix of CF and NCF systems in the two samples (5 and 4 NCFs in the low and high redshift samples, respectively). The mean metallicities for the low- z and high- z samples (using spectral model A for all clusters) are 0.30 ± 0.08 and 0.31 ± 0.09 , respectively. The application of the Student's t-test shows the difference between the mean metallicities for the high- z and low- z samples to be significant at only the 18 per cent confidence level. In agreement with Mushotzky and Lowenstein (1997) we therefore find no evidence for evolution in the emission-weighted metallicities over the range of redshifts covered by our study. We also note that we find no evidence for significant evolution in the X-ray gas mass fraction, with a mean value for both the low and high redshift subsamples of 0.16.

4 DISCUSSION

4.1 Metallicity gradients, mergers and mixing

Fabian *et al.* (1994a) suggested that the higher emission-weighted metallicities for CF clusters could be due to inhomogeneities in the ICM, with small blobs of cooler, denser and more metal-rich gas being immersed in hotter gas at the centres of the CF systems. The distributed mass deposition profiles within cooling flows requires that the ICM there is inhomogeneous (Fabian 1994 and references therein). Fabian

et al. (1994a) also noted the potential importance of abundance gradients in clusters. Abundance gradients appear to be a common feature of the cores of CF clusters. First noticed in ASCA (Fukazawa *et al.* 1994) and ROSAT PSPC (Allen & Fabian 1994) spectra of the Centaurus cluster, an increase in the iron abundance towards the centres of CF clusters has since been found in ASCA spectra for Abell 496 (Hatsukade 1997), the Virgo cluster (Matsumoto *et al.* 1996) and AWM7 (Ezawa *et al.* 1997). The abundance of iron across the Perseus cluster, which also hosts a large cooling flow, appears patchy with the highest value probably occurring in the core (Arnaud *et al.* 1994; see also Molendi *et al.* 1998). In contrast, ASCA studies of Abell 1060 (Tamura *et al.* 1996), the Ophiuchus cluster (Matsuzawa *et al.* 1996) and the Coma Cluster (Watanabe *et al.* 1997), which have little or no cooling flows, show no abundance gradients.

An abundance gradient will strongly influence the emission-weighted metallicity determined from the integrated X-ray spectrum of a cluster. The X-ray emission depends on the square of the ICM density and so is dominated by the innermost, densest regions of a cluster. This is particularly the case for CF clusters, where a significant fraction (up to ~ 70 per cent) of the total X-ray luminosity may arise from within the central 2–3 hundred kpc (Peres *et al.* 1997; Allen *et al.* 1998). We have simulated the effects of metallicity gradients on the mean emission-weighted metallicities for CF and NCF clusters using the observed X-ray surface brightness profiles for Abell 478 and 2218 as representative examples of CF and NCF systems. (These clusters have the highest-quality imaging data.) We find that a linear gradient in metallicity dropping from ~ 0.8 solar at the centre to ~ 0.1 solar at 500 kpc (and remaining roughly constant outside this radius) leads to a mean emission-weighted metallicity, for a CF cluster like Abell 478, of about 0.4. For a NCF system, for which the X-ray surface brightness profile will be much less sharply-peaked, the mean emission-weighted metallicity will be only ~ 0.2 . Such gradients should be easily detectable with AXAF.

The abundance gradient model provides the most natural explanation for the segregation in the metallicity results for the CF and NCF clusters. The metal-rich core may be the oldest part of a cluster, forming earliest in the deep potential wells. This could enhance both the formation of massive stars and the retention of gas in these regions. (We note that many of the most-massive CF clusters also show evidence for ongoing star formation in their cores; *e.g.* Allen 1995). After their initial collapse, clusters continue to evolve by the accretion of material, often via subcluster merger events. NCF clusters, such as those included in this study, are thought to have recently experienced a major merger event wherein a large mass component has strongly interacted with the cluster core (Allen 1998). Such events will significantly disrupt the X-ray gas in the core regions of the clusters and will mix and spread the central high-metallicity gas with the outer less metal-rich material. The abundance gradients in NCF clusters are thereby reduced (or even destroyed), although the *total* mass of metals in the ICM is unchanged. (An implication of this is that the global metallicity of the ICM is more accurately estimated for the NCF systems, where the metals are more evenly mixed with the cluster gas.) The dependence of cluster metallicities on the presence or absence of a cooling flows then reflects whether these systems have

had their core regions left undisturbed, or recently mixed, rather than on any internal property of the cooling flows such as their mass deposition rates.

Reisenegger *et al.* (1996) have suggested that the abundance gradient in the Centaurus cluster could result from the cooling flow in that cluster concentrating the metals ejected by type-Ia supernovae in the outer regions of the cD galaxy. Although this mechanism is plausible for low-luminosity systems like the Centaurus cluster, with relatively high ratios of the stellar mass in the central galaxy to the X-ray gas mass, it has more difficulty in accounting for the gradients in more X-ray luminous clusters, with lower stellar/X-ray gas mass ratios. This implies that the metallicity gradients in luminous CF clusters may have been present since some early epoch in their formation history.

A further possibility to explain the metallicity gradients in cooling-flow clusters is that most of the metals in cluster cores may reside in large grains. The lifetime of grains of radius $a\mu\text{m}$ to sputtering in hot gas of density n is $\sim 2 \times 10^6 a/n\text{yr}$ (Draine & Salpeter 1979). Provided that individual grains exceed $10\mu\text{m}$ in radius, they should survive for a Hubble time or longer throughout NCF objects and beyond the cooling radius in clusters with cooling flows. Within cooling flows, the density rises inward so the grains are increasingly sputtered, releasing the metals into the gas phase which thus becomes increasingly metal rich toward the cluster centre. Such a model requires that about half the metals are originally injected into the ICM as large grains. We note that large grains are inferred to have formed and to carry most of the iron in the expanding remnant of SN1987A (Colgan *et al.* 1994). Within this model the typical mean metallicity in the *core* of a cluster would be 0.5–1.0 solar. The grains would also provide a possible source for the dust inferred in the central optical nebulosities in cooling flows (Fabian, Johnstone & Daines 1994b; Voit & Donahue 1995; Allen *et al.* 1995) and may be related to the excess soft X-ray absorption observed in cooling flows (*e.g.* Allen & Fabian 1997).

4.2 The effects of cluster evolution

Within standard formation scenarios, clusters that form earlier are expected to have higher luminosities for a given temperature (since the gas density is higher at earlier formation epochs). Scharf & Mushotzky (1997) presented results from a single-temperature analysis of ~ 30 clusters observed with ASCA and demonstrated a positive correlation between the amplitude, A_{LT} , of the $L_X - T_X$ relation (where they define $L_X = A_{\text{LT}} T_X^3$) and the mean (emission-weighted) metallicity. They suggest that the origin of this correlation is that clusters with larger values of A_{LT} formed earlier and were better able to hold on to the metal-enriched gas expelled from their galaxies. Assuming that metals cannot be lost from the cluster potentials without a corresponding decrease in the X-ray gas mass, clusters with lower A_{LT} should have lower baryon fractions by about a factor of two, given the observed range in metallicities.

The Table lists the baryon fractions at a radius of 500 kpc in the clusters, determined with the appropriate spectral models (spectral model C for the CF systems and model A for the NCFs). We see that the mean baryon fractions for the subsamples of CF and NCF clusters differ by only ~ 30

per cent, and thus that relatively little gas has escaped the potentials of the NCF clusters relative to the CF systems. (We note, however, that the distributions of baryon fraction values for the CF and NCF clusters are different. The application of a Student's t-test shows the mean values for the two subsamples to differ at > 99 per cent confidence. The NCF clusters also have a significantly smaller dispersion in baryon fractions than the CF systems, and a Kolmogorov-Smirnov test shows the two subsamples to be drawn from different populations at > 99 per cent significance.) If spectral model B rather than model A is used for the NCF systems (*i.e.* if the absorbing column density is included as a free parameter in the spectral analysis of the NCF systems) the mean baryon fraction for these clusters rises to 0.16, improving the agreement with the CF clusters.

It is important to note that the clusters studied in this Letter are amongst the most X-ray luminous and by implication most-massive clusters known. Material expelled from their member galaxies, even when part of an early low-mass subclump, is unlikely to escape from the total cluster potential. The accompanying Letter (Allen & Fabian 1998) discusses the impact of cooling flows on the $L_{\text{Bol}} - T_{\text{X}}$ relation for clusters. Allen (1998) discusses the effects of cooling flows on X-ray mass measurements. The new data presented in this Letter reveal a link between cooling flows and metallicity measurements and suggest the presence of metallicity gradients in clusters with cooling flows. Such effects must be accounted for before attempting to determine cosmological parameters from X-ray observations of clusters.

ACKNOWLEDGMENTS

We thank the Royal Society for support.

REFERENCES

- Allen S.W., 1995, MNRAS, 276, 947
 Allen S.W., 1998, MNRAS, in press (astro-ph/9710217)
 Allen S.W., Fabian A.C., 1994, MNRAS, 269, 409
 Allen S.W., Fabian A.C., 1997, MNRAS, 286, 583
 Allen S.W., Fabian A.C., 1998, MNRAS, submitted
 Allen S.W., Fabian A.C., Edge A.C., Böhringer H., White D.A., 1995, MNRAS, 275, 741
 Allen S.W. *et al.* 1998, in preparation
 Anders E., Grevesse N., 1989, *Geochemica et Cosmochimica Acta* 53, 197
 Arnaud M., Rothenflug R., Boulade O., Vigroux L., Vangioni-Flam E., 1992, *A&A*, 254, 49
 Arnaud K.A., 1996, in *Astronomical Data Analysis Software and Systems V*, eds. Jacoby G. and Barnes J., ASP Conf. Series volume 101, p17
 Arnaud K.A. *et al.* , 1994, *ApJ*, 436L, 67
 Balucinska-Church M., McCammon D., 1992, *ApJ*, 400, 699
 Colgan S.W., Haas M.R., Erickson E.F., Lord S.D., Hollenbach D.J., 1994, *ApJ*, 427, 874
 David L.P., Jones C., Forman W., 1995, *ApJ*, 445, 578
 Dickey J.M., Lockman F.J., 1990, *ARA&A*, 28, 215
 Draine B.T., Salpeter E.E., 1979, *ApJ*, 231, 77
 Edge A.C., Stewart A.C., 1991, MNRAS, 252, 414
 Edge A.C., Stewart G.C., Fabian A.C., 1992, MNRAS, 255, 431
 Ezawa H., Fukazawa Y., Makishima K., Ohashi T., Takahara F., Xu H., Yamasaki N.Y., 1997, preprint, astro-ph/970928
 Fabian A.C., 1994, *A&AR*, 32, 277
 Fabian A.C., Johnstone R.M., Daines S.J., 1994b, MNRAS, 271, 737
 Fabian A.C., Crawford C.S., Edge A.C., Mushotzky R.F., 1994a, MNRAS, 267, 779
 Fukazawa Y., Ohashi T., Fabian A.C., Canizares C.R., Ikebe Y., Makishima K., Mushotzky R.F., Yamashita K., 1994, PASJ, 46L, 55
 Hatsukade I., Kawarabata K., Takenada K., Ishizaka J., 1997, in Makino F., Mitsuda K., eds., *X-ray Imaging and Spectroscopy of Cosmic Hot Plasmas*, Universal Academy Press, Tokyo, p. 105
 Johnstone R.M., Fabian A.C., Edge A.C., Thomas P.A., 1992, MNRAS, 255, 431
 Kaastra J.S., Mewe R., 1993, *Legacy*, 3, HEASARC, NASA
 Kauffmann G., Charlot S., 1997, preprint, astro-ph/9704148
 Kowalski M.P., Cruddace R.G., Snyder W.A., Fritz G.G., Ulmer M.P., Fenimore E.E., 1993, *ApJ*, 412, 489
 Matsumoto H., Koyama K., Awaki H., Tomida H., Tsuru T., Mushotzky R., Hatsukade I., 1996, PASJ, 48, 201
 Matsuzawa H., Matsuoka M., Ikebe Y., Mihara T., Yamashita K., 1996, PASJ, 48, 565
 Molendi S., Matt G., Antonelli L.A., Fiore F., Fusco-Femiano R., Kaastra J., Maccarone C., Perola C., 1998, *ApJ*, in press (astro-ph/9802067)
 Mushotzky R.F., Lowenstein M., 1997, *ApJ*, 481L, 63
 Mushotzky R.F., Lowenstein M., Arnaud K.A., Tamura T., Fukazawa Y., Matsushita K., Kikuchi K., Hatsukade I., 1996, 466, 686
 Peres C.B., Fabian A.C., Edge A.C., Allen S.W., Johnstone R.M., White D.A., 1997, MNRAS, in press
 Press W.H., Teukolsky S.A., Vetterling W.T., Flannery B.P., 1992, *Numerical Recipes*, Cambridge University Press
 Reisenegger A., Miralda-Escué J., Waxman E., 1996, *ApJ*, 457, 11L
 Scharf C.A., Mushotzky R.F., 1997, *ApJ*, 485L, 65
 Tamura T. *et al.* , 1996, PASJ, 48, 671
 Voit G.M., Donahue M., 1995, *ApJ*, 452, 164
 Watanabe M., Yamashita K., Kunieda H., Tawara Y., 1997, in Makino F., Mitsuda K., eds., *X-ray Imaging and Spectroscopy of Cosmic Hot Plasmas*, Universal Academy Press, Tokyo, p. 131
 White D.A., Fabian A.C., 1995, MNRAS, 273, 72
 White R.E. III, Day C.S., Hatsukade I., Hughes J.P., 1994, *ApJ*, 433, 583
 Yamashita K., 1992, in Tanaka Y., Koyama K., eds, *Frontiers of X-ray Astronomy*, Universal Academy Press, p. 475